On the electrodynamics of semiconductor magnetoplasmic waveguides

© M.V. Davidovich

Saratov National Research State University,
410012 Saratov, Russia

E-mail: davidovichmv@info.sgu.ru

Received February 21, 2024
Revised June 20, 2024
Accepted August 21, 2024

The dispersion of magnetoplasmons propagating along the surface of a metamaterial with periodic well-conducting semiconductor or metallic inclusions under the application of a strong external magnetic field along the propagation direction is considered. The tensor of the effective dielectric constant of a metamaterial in the presence of a field is found on the basis of the effective medium method. It is shown that in the THz range there are delayed magnetoplasmons with low losses, i.e. such a structure with a flat surface behaves like a decelerating system and can be used in an TWT with magnetic induction of the order of 1Tl, which is necessary for focusing a ribbon electron beam. The magnetic field effectively controls the dispersion.

Keywords: magnetoplasmon, THz TWT, dispersion, hyperbolic metamaterial, homogenization, dispersion equations.

DOI: 10.61011/SC.2024.06.59449.6062

1. Introduction

Magnetoplasmons (MPs) are electromagnetic waves propagating along the surfaces of waveguide structures with conducting elements in an external constant magnetic field $\mathbf{H}_0$. It may be directed normal or tangential to the surface or be oriented at an arbitrary angle to it. One may control the MP dispersion by adjusting the direction and magnitude of $\mathbf{H}_0$. In the present study, we consider a surface waveguide of this kind with a tangential magnetic field co-directional with the motion of an MP (Figure 1) with dependence $\exp(i\omega t - ik_z z)$. This MP may be excited effectively by a ribbon electron beam if its velocity is close to the MP phase velocity. The MP then interacts effectively with such a beam and may be amplified by it, which is relevant to the design of traveling-wave amplifiers (e.g., TWTs operating in the EHF and THz ranges). Decelerations n on the order of several units are needed in this case. The excitation of an MP by relativistic electron beams may be detected if the magnetic field is switched off at some point or a prism is installed so that the MP becomes leaky.

The simplest plasmon waveguide is a highly conducting thin plate with a surface wave [1]. The plate may be metallic or semiconducting, and plasmon polaritons (PPs) propagate along its surfaces. Very slow PPs are of interest, and a thin layer is needed to obtain them. The maximum of n' shifts to the low-frequency region as the thickness decreases. It is hard to reduce the thickness to less than a few nanometers, since the film becomes discontinuous. Semiconductor films with their plasma frequencies (PFs) ω_p being way below those of metals are promising. When a magnetic field is applied, cyclotron frequencies (CFs) ω_H emerge, and the deceleration may increase significantly. The Larmor CF in copper at 1 T is $\omega_H = 176$ GHz. Owing to a low effective mass, CFs in semiconductors fall within the THz range. PFs may be shifted into the same range by doping and adjusting the temperature. The collision rate (CR) may be made significantly lower than ω_p and ω_H, which makes semiconductor materials promising for observation of slow MPs. If one of the transverse dimensions is large (strictly speaking, infinite; e.g., the y dimension in Figure 1), the problem for a homogeneous plate with and without a magnetic field is solved analytically. The fields do not depend on y in this case, and the field of a slow surface MP or PP decreases in direction $\pm x$ away from the surface. The waves for fast MPs are leaky. The tensor dielectric constant (DC) of semiconductor plasma in a magnetic field should be used for MPs. In the general case of an inhomogeneous or finite plate, the problem is formulated as a one-dimensional integral equation (IE) with respect to the distribution of the transverse electric field [2]. It is theoretically possible to obtain explicit dispersion equations (DEs) for plane-layered structures with homogeneous metallic or dielectric layers [1]. It should be noted that rigorous quantum approaches (e.g., the density functional method [3] and nonequilibrium Green's functions [4]) have not been applied in the study of MPs; they were used only to obtain static conductivities of thin films. MPs in conducting semiconductor films were examined in [5–9]. The case with surface MPs propagating perpendicular to the magnetic field, which was discussed in [5], differs from the one considered in the present study. The MP excitation was studied in [6–9]. Dispersion equations of MPs propagating in a thin conducting film along the magnetic field were analyzed in [10]. The properties of macroscopic conducting elements differ greatly (especially in terms of conductivity [11]) from those of elements that are small compared to the mean free path of electrons, which is due mostly to a strong CR increase attributable to the influence of boundaries. However, Larmor radius $r_L = E_0/(B_{0z}\omega)$ is rather small in strong magnetic field H_{0z} at the examined high frequencies and moderate electric field magnitudes E_0;

therefore, one may use the classical DC of magnetized semiconductor plasma, which is what is considered below.

Structures of the type shown in Figure 1 are promising for MPs, since they allow one to alter dispersion by adjusting the configuration. In what follows, we assume that $a = t$ and one dimension is greater than the other ($a \gg b$), applying homogenization for a layer of metamaterial finite in x (Figure 1) with semiconductor inclusions in a dielectric under the influence of external magnetic field $\mathbf{B} = \mathbf{z}_0\mu_0 H_0$. It serves to focus the ribbon electron beam and has a strong effect on the MP deceleration. It is hard to use a solid metal plate directly, since the PF of metals is significantly higher than the CF. In addition, the CR for metals falls within the THz range at room temperature, which precludes one from obtaining significant decelerations at low losses. The structure shown in Figure 1, b (the one with round wires) makes it possible to reduce the effective PFs by more than 2 orders of magnitude. Assuming that their radius $r < 0.17d$, a reduction of 4 orders of magnitude (or more) is achieved at $r < 0.0056d$. With wavelength $\lambda = 0.3$ mm, we obtain an acceptable homogenization period $d = 3\,\mu$m and radius $r = 17$ nm. The effective PF then falls within the THz range, and the CR decreases by several orders of magnitude. In a magnetic field, the corresponding MPs are weakly magnetic in nature and may be regarded as magnetically disturbed electric E-PPs with reduced plasmon resonance frequencies.

Structures similar to those shown in Figure 1, a correspond to MPs. They were investigated in [12]. The approach used by the authors of this study differs slightly from the one applied below; the coefficient of reflection from a metamaterial layer was examined, while MPs were not analyzed. In zero magnetic field, the structures illustrated in Figure 1 may act as hyperbolic metamaterials (HMMs) in certain frequency ranges [13]. The PP dispersion along HMM layers and the calculation of coefficients of reflection and transmission for such layers (including those with a rotated anisotropy axis) were discussed in [14,15]. When a magnetic field is applied, these structures turn into biaxial artificial media (photonic crystals) and may exhibit a number of novel properties (including wave-type conversion and nonreciprocity) upon diffraction [15]. Structures of the type shown in Figure 1 may be classified as wire metamaterials (wire media). They were examined in, e.g., [16–24], where the properties of HMMs and ENZ (epsilon-near-zero) metamaterials [25] were demonstrated, and continue to attract attention [13]. The electrodynamics of such media is commonly analyzed based on the Fresnel equation (FE) only without due regard to spatial dispersion (SD). The wide range of application of these metamaterials necessitates the development of rigorous electrodynamic models, which is made possible by the IE method that allows for proper characterization of SD. The SD in such media is significant even at low frequencies [16]. However, when MPs propagate along the wires (in the present case, at $k_y = 0$), the SD may be neglected. The application of a magnetic field, especially a field with arbitrary spatial orientation, makes DEs obtained on the basis of rigorous approaches

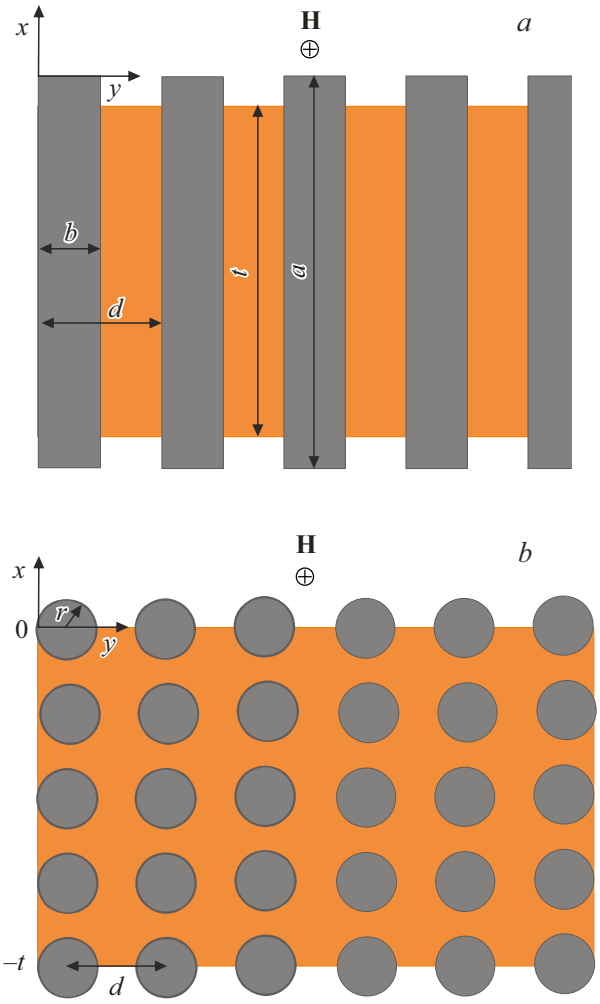

Figure 1. Plasmon waveguide structures with rectangular (a) and round semiconductor or metallic inclusions cylindrical along the z axis (b).

significantly more complicated, while the approach used below is rather simple.

The aim of the present study is to examine the MP dispersion along the boundaries of a metamaterial layer with semiconductor and metallic inclusions (Figure 1) in an external magnetic field and obtain the corresponding results for a continuous thin semiconductor plate. Since dispersion curves have a complex shape with alternating slow and fast branches, the goal is to determine the frequencies of the fastest waves and the characteristic transition frequencies at which deceleration n is equal to unity. The slowest branches lie in the regions between two closest points with $n = 1$ that contain no points of fast waves with $n \approx 0$.

2. Effective DC method and dispersion equations

The derivation of DEs for the structures shown in Figure 1 by the IE method is a rather complex numerical

problem, which then needs to be solved numerically multiple times to obtain complex roots. Since inclusions are several orders of magnitude smaller than the considered THz wavelengthsλ, we use homogenization based on the Garnett formula to obtain an effective DC at $d \ll \lambda$. The concentration of conducting inclusions for the structures in Figure 1, *a* is $\delta = b/d$ and may be small or on the order of 1. The structure presented in Figure 1, *a* has the advantage that the ε_{xx} component produces a significant contribution to the MP properties. Depolarization coefficient $L_z = 0$ for this structure, and the sum of the other two coefficients is unity. Let us set $L_x = b/a \ll 1$, $L_y = 1 - b/a$. The following modified Garnett formula ($k = x, y, z$) is then obtained for the effective DC components:

$$\frac{\varepsilon_{kk} - \varepsilon_d}{L_k(\varepsilon_{kk} - \varepsilon_d) + \varepsilon_d} = \delta \frac{\varepsilon - \varepsilon_d}{\tilde{\varepsilon} + L_k(\varepsilon - \varepsilon_d)}.$$

Rewriting it for three diagonal tensor components, we find

$$\begin{aligned}
\varepsilon_{xx} &= \varepsilon_d \frac{\varepsilon_d + L_x(\varepsilon - \varepsilon_d) + \delta(1 - L_x)(\varepsilon - \varepsilon_d)}{\varepsilon_d + L_x(\varepsilon - \varepsilon_d) - \delta L_x(\varepsilon - \varepsilon_d)} \\
&\approx \varepsilon_d[1 + \delta(\varepsilon/\varepsilon_d - 1)], \\
\varepsilon_{yy} &= \varepsilon_d \frac{\varepsilon_d + L_y(\varepsilon - \varepsilon_d) + \delta(1 - L_y)(\varepsilon - \varepsilon_d)}{\varepsilon_d + L_y(\varepsilon - \varepsilon_d) - \delta L_y(\varepsilon - \varepsilon_d)} \\
&\approx \varepsilon_d \frac{\varepsilon}{\varepsilon - \delta(\varepsilon - \varepsilon_d)} \approx \varepsilon_d - \delta\varepsilon_d(1 - \varepsilon_d/\varepsilon), \\
\varepsilon_{zz} &= \varepsilon_d + \delta(\varepsilon - \varepsilon_d). \qquad (1)
\end{aligned}$$

Applying the Rytov formula [26] at $a \to \infty$, we obtain $\varepsilon_{xx} = \varepsilon_{zz} = \varepsilon_d(1-\delta) + \delta\varepsilon$, $\varepsilon_{yy} = \varepsilon_d/[1 - \delta(1 - \varepsilon_d/\varepsilon)] \approx \varepsilon_{yy} = [(1 - \delta)/\varepsilon_d + \delta/\varepsilon]^{-1} \approx \varepsilon_d - \varepsilon_d\delta(1 - \varepsilon_d/\varepsilon)$, which corresponds to (1). The corresponding Bruggeman formula with depolarization coefficients takes the form

$$\delta \frac{\varepsilon_{kk} - \varepsilon}{\varepsilon_{kk} + L_k(\varepsilon - \varepsilon_{kk})} + (1 - \delta) \frac{\varepsilon_{kk} - \varepsilon_d}{\varepsilon_{kk} + L_k(\varepsilon_d - \varepsilon_{kk})} = 0.$$

The longitudinal component is $\varepsilon_{zz} = \varepsilon_d + \delta(\varepsilon - \varepsilon_d)$, which is the same as (1). Quadratic equations are obtained for transverse components. Specifically,

$$\varepsilon_{xx} = \frac{L_x\{\varepsilon\delta[\varepsilon_d + (1 - \delta)\varepsilon] - (1 - \delta)\varepsilon_d\varepsilon\} - \varepsilon_{xx}^2}{\delta L_x\varepsilon_d - \varepsilon\delta(1 - L_x) - (1 - \delta)(1 - L_x)\varepsilon_d}. \qquad (2)$$

One root corresponds to a physical solution. The first term in curly brackets in the numerator of (2) is small. Dropping it, we obtain approximate solution $\varepsilon_{xx} = (1 - L_x)[\varepsilon\delta + (1 - \delta)\varepsilon_d] - \delta L_x\varepsilon_d$. It matches (1) at $L_x \to 0$. However, it may be refined by inserting into the right-hand side of (2) (i. e., by taking one iteration). In the second structure (Figure 1, *b*) with spherical inclusions, all depolarization coefficients are equal to 1/3, and the Garnett formula yields an isotropic medium with effective DC

$$\varepsilon_{ef} = \varepsilon_d \frac{1 + 2\delta(\varepsilon - \varepsilon_d)/(\varepsilon + 2\varepsilon_d)}{1 - \delta(\varepsilon - \varepsilon_d)/(\varepsilon + 2\varepsilon_d)} \approx \varepsilon_d\left(1 + 3\delta \frac{\varepsilon - \varepsilon_d}{\varepsilon + 2\varepsilon_d}\right). \qquad (3)$$

In formula (3), $\delta = 4\pi r^3/(3d^3) \ll 1$. When the inclusions are infinite cylinders, $\delta = \pi r^2/d^2 \ll 1$, $L_x = L_y = 1/2$, $L_z = 0$. Then, $\varepsilon_{xx} = \varepsilon_{yy} = \varepsilon_\perp$, $\varepsilon_{zz} = \varepsilon_\parallel$, and

$$\begin{aligned}
\varepsilon_\perp &= \varepsilon_d \frac{1 + \delta(\varepsilon - \varepsilon_d)/(\varepsilon + \varepsilon_d)}{1 - \delta(\varepsilon - \varepsilon_d)/(\varepsilon + \varepsilon_d)} \\
&\approx \varepsilon_d[1 + 2\delta(\varepsilon - \varepsilon_d)/(\varepsilon + \varepsilon_d)], \\
\varepsilon_\parallel &= \varepsilon_d + \delta(\varepsilon - \varepsilon_d). \qquad (4)
\end{aligned}$$

This medium of metal cylinders may be an HMM in two-frequency ranges: $\varepsilon_\parallel\varepsilon_\perp < 0$ (with losses neglected). The DC in the Drude–Lorentz form in zero magnetic field is $\varepsilon = \varepsilon_L - \omega_p^2(\omega^2 - i\omega\omega_c)$, but turns into a tensor when a magnetic field is applied:

$$\begin{aligned}
\varepsilon_{xx}(\omega) &= \varepsilon_{yy}(\omega) = \varepsilon_\perp = \varepsilon_L - \frac{\omega_p^2}{\omega^2 - \omega_H^2 - i\omega\omega_{co}}, \\
\varepsilon_{xy}(\omega) &= -\varepsilon_{yx}(\omega) = \frac{-i\omega_p^2\omega_H}{\omega(\omega^2 - \omega_H^2 - i\omega\omega_{co})} = -i\beta, \\
\varepsilon_{zz}(\omega) &= \varepsilon(\omega) = \varepsilon_L - \frac{\omega_p^2}{\omega^2 - i\omega\omega_{co}}. \qquad (5)
\end{aligned}$$

Here, $\omega_p^2 = N_e e^2/(\varepsilon_0 m_e^*)$ is the PF, $\omega_H = \mu_0 H_0 e/m_e$ is the CF, ω_{co} is the CR, ε_L is the Lorentz term, and m_e is the effective electron mass. In metals, term ε_L remains almost unchanged and real up to optical frequencies. One may set $\varepsilon_L = 9.3$, $\omega_p = 1.57 \cdot 10^{16}$ Hz for silver. At 300 K, $\omega_{co} = 3.56 \cdot 10^{13}$ Hz for silver. These values were obtained with account for the electron concentration, the experimental value of direct-current conductivity, and the experimental value of zero-crossing frequency of the real DC part [27]. In copper, $\varepsilon_L = 13.09$, $\omega_p = 1.65 \cdot 10^{16}$ Hz, and $\omega_c = 4.23 \cdot 10^{13}$ Hz. The CR for metals is inversely proportional to temperature, while concentration N_e and the PF are virtually independent of it. At a temperature on the order of 1 K, one may set $\omega_{co} \sim 10^{11}$ Hz. Extremely strong magnetic fields and cryogenic temperatures are needed to obtain slow MPs in metallic structures in the THz range. A high PF makes a uniform metal layer with DC (3) a rather bad MP waveguide in the THz range [10]. Therefore, semiconductor structures are more convenient. We use the relation of concentration with temperature and bandgap for such structures. Concentrations and PFs are low at low temperatures. The PF may be altered by doping. With heavy doping, the PF depends only weakly on temperature. The following materials may be convenient: heavily doped indium antimonide *n*-InSb ($\varepsilon_L = 17.0$, effective electron mass $m_e^* = 0.013m_e$, and an electron mobility of $1.1 \cdot 10^6$ cm^2/(V·s) at $T = 77$ K); *n*-GaAs doped with silicon ($\varepsilon_L = 14.0$, $m_e^* = 0.067m_e$, and an electron mobility of 8500 cm^2/(V·s) at 300 K); and zero-gap mercury telluride HgTe (with an electron concentration of 10^{21} m^{-3}, an effective mass of $0.013m_e$, and a mobility of 10^8 cm^2/(V·s) at $T = 4.2$ K [28]). The structures shown in Figure 1 are convenient in that they allow one to

adjust the effective PF, CR, and CF without the use of low temperatures. Effective DC (3) of the metamaterial has reduced effective PF and CR. The effective cyclotron frequency also decreases. Therefore, the effect of a magnetic field on the structure shown in Figure 1, *b* is weaker than the corresponding effect on a solid semiconductor. The influence of low temperatures in metals is manifested primarily in a CR reduction. In the case of semiconductors, the concentration and, accordingly, the PF and CR decrease sharply. Since the PF may then become very low, doping is needed to raise the concentration and obtain a PF in the THz range. As for the cyclotron frequency, it falls within the THz range at an effective mass on the order of $0.01-0.1$ of the electron mass and an induction of 1 T. The $\varepsilon_\perp$ value from (5) should be used instead of ε in formula (4) for $\varepsilon_\perp$; the formula for $\varepsilon_\parallel$ remains unchanged. The same is true for formula (3), which also becomes tensorial when a magnetic field is applied.

If a magnetic field is applied to a structure with DC (1), we use the effective DC components denoted with a tilde that are given in the *Appendix* (formula (A.1)). Using Maxwell's equations (formulae (A.2)–(A.12) from the *Appendix*), we obtain a DE [1] for a layer that splits into two equations:

$$\frac{k_{x\pm}/k_{0x}+\tilde{\varepsilon}_{zz}}{k_{x\pm}/k_{0z}+\tilde{\varepsilon}_{zz}}=\pm\psi, \tag{6}$$

$$\frac{k_{x\pm}/k_{0x}+1}{k_{x\pm}/k_{0x}-1}=\pm\psi, \tag{7}$$

where $\psi=\exp(-ik_{x\pm}t)$. One may also write $k_{x\pm}=$ $=\tilde{\varepsilon}_{zz}k_{0x}[-i\tan(k_{x\pm}t/2)]^{\pm1}$. Equation (7) is derived from (6) by performing the $\tilde{\varepsilon}_{zz}\to 1$ substitution. Here, $k_{0x}=\sqrt{k_0^2-k_z^2}$ for vacuum. At a large thickness t and with even an infinitely weak dissipation, $\psi=0$; therefore, $k_{x\pm}+\tilde{\varepsilon}_{zz}\sqrt{k_o-k_z}=0$. We simplified the problem under the assumption that the metamaterial layer is thick (in these conditions, the wave reflected from the far boundary may be neglected). The $k_{x\pm}$ quantities are the roots of FE (A.5) such that $\mathrm{Im}\left(\sqrt{B\pm D}\right)<0$. This implies that wave $\exp(-ik_{x\pm}x)$ decays toward positive x. This also means that the square of the given quantity is $K_{x\pm}^2=k_{x\pm}^{\prime 2}-k_{x\pm}^{\prime\prime 2}-2ik_{x\pm}^{\prime}k_{x\pm}^{\prime\prime}$ and has an imaginary part with its sign specified by the sign of $k_{x\pm}^{\prime}$. For a forward wave along the x axis, $k_{x\pm}^{\prime}k_{x\pm}^{\prime\prime}>0$; for a backward wave, $k_{x\pm}^{\prime}k_{x\pm}^{\prime\prime}<0$. In vacuum at $x>0$, the fields are written as $E_y(x)=E_{0y}^{+}\exp(-ik_{0x}x)$, $h_z(x)=y_{0h}E_{0y}^{+}\exp(-ik_{0x}x)$, $E_z(x)=E_{0z}^{+}\exp(-ik_{0x}x)$, $h_y(x)=-y_{0e}E_{0z}^{+}\exp(-ik_{0x}x)$. Here, $y_{0e}=k_0/k_{0x}=1/n_{0x}$ and $y_{0h}=k_{0x}/k_0=n_{0x}=\sqrt{1-n_z^2}$. Sewing the fields together at $x=0$, we obtain DE $(\beta_{zx}-y_{0h}\rho_{hz})(y_{0e}\alpha_{zx}-y_{ez}=0$. It splits into two equations: $y_{0e}=y_{ez}/\alpha_{zx}$ and $y_{0h}=\beta_{zx}/\rho_{hz}$. The second one yields $\sqrt{1-n_z^2}=-n_x$ or $n_z^2=1-n_x^2$. Here, $n_{x\pm}=k_{x\pm}/k_0$ and $n_z=n=k_z/k_0$ are complex decelerations. For ease of classification, waves with an infinitely weak dissipation are considered below. A finite dissipation is taken into account in numerical calculations. For a non-dissipative MP to be slow, $n_{x\pm}^2$ should be a negative quantity, and $k_{x\pm}$ must be imaginary and large in magnitude. This wave is a surface one. At large decelerations and zero dissipation, $n=k_z/k_0\gg 1$, $B\approx -k_z^2(1+\tilde{\varepsilon}_{zz}/\tilde{\varepsilon}_{xx})/2$, and $C\approx k_z^4\tilde{\varepsilon}_{zz}/\tilde{\varepsilon}_{xx}$. Therefore, $k_{x\pm}^2\approx[-k_z^2(1+\tilde{\varepsilon}_{zz}/\tilde{\varepsilon}_{xx})\pm k_z^2(1-\tilde{\varepsilon}_{zz}/\tilde{\varepsilon}_{xx})]/2$. Taking the upper sign in the root value, we find $k_{x+}^2\approx k_z^2\tilde{\varepsilon}_{zz}/\tilde{\varepsilon}_{xx}$. if $\tilde{\varepsilon}_{zz}/\tilde{\varepsilon}_{xx}>0$, waves within the layer have dependences $\exp(\mp ik_{x\pm}x)$; if $\tilde{\varepsilon}_{zz}/\tilde{\varepsilon}_{xx}<0$, the dependences are exponential: $\exp\left(\mp k_z x\sqrt{|\tilde{\varepsilon}_{zz}/\tilde{\varepsilon}_{xx}|}\right)$. In the metamaterial half-space, the fields decrease from the boundary toward negative x; i. e., only the $\exp\left(k_z x\sqrt{|\tilde{\varepsilon}_{zz}/\tilde{\varepsilon}_{xx}|}\right)$ wave should remain. Inequality $\tilde{\varepsilon}_{zz}\geq-\tilde{\varepsilon}_{xx}$ should hold at large decelerations. Taking the upper sign in the root value, we obtain $k_{x-}^2\approx -k_z^2$. A slow wave then also decays in the structure as $\exp(k_z x)$. Two branches of the $k_z^2=k_0^2-B\mp D$ FE should be used in numerical calculations. In the case of the first DE, $1/\sqrt{1-n_z^2}=-\tilde{\varepsilon}_{zz}/n_{x\pm}$, which yields $n_z^2=1-(n_{x\pm}/|\tilde{\varepsilon}_{zz}|)^2$. If a wave is very slow, the quantity in brackets must be imaginary and large in magnitude. The $\tilde{\varepsilon}_{zz}$ quantity may be imaginary and large in magnitude at very low frequencies. At frequencies typical of plasmonics, one may assume that $\tilde{\varepsilon}_{zz}<0$. Using the first approximate root, we obtain $n_z^2\approx 1-n_z^2/(\tilde{\varepsilon}_{zz}\tilde{\varepsilon}_{xx})$. Naturally, $(\tilde{\varepsilon}_{zz}\tilde{\varepsilon}_{xx})\approx -1$ should hold. With zero dissipation, we get $\varepsilon<0$ at $\omega<\omega_p/\sqrt{\varepsilon_L}$ and $\varepsilon_\perp<0$ at $\omega_H<\omega<\sqrt{\omega_H^2+\omega_p^2/\varepsilon_L}$. In such a case, $(\varepsilon-\varepsilon_d)(\varepsilon_\perp-\varepsilon_d)>0$, and the following is needed to fulfill the condition:

$$\delta\approx\frac{\varepsilon_d^2+\delta^2(\varepsilon-\varepsilon_d)(\varepsilon_\perp-\varepsilon_d)+1}{(2\varepsilon_d-\varepsilon-\varepsilon_\perp)\varepsilon_d}.$$

Using the second approximate root, we obtain $n_z^2\approx 1+n_z^2/\tilde{\varepsilon}_{zz}^2$. This condition should correspond to $\tilde{\varepsilon}_{zz}\approx 1$ or $\omega\approx\omega_p\sqrt{\delta}/\sqrt{\varepsilon_d-1+\delta(\varepsilon_L-\varepsilon_d)}$.

To obtain more precise formulae for dispersion at large decelerations, one needs to take into account the next terms in the representation of quantities B and C: namely, $B=B_0+\Delta B$, $C=C_0+\Delta C$, $B_0=-k_z^2(1+\tilde{\varepsilon}_{zz}/\tilde{\varepsilon}_{xx})/2$, $C_0=k_z^4\tilde{\varepsilon}_{zz}/\tilde{\varepsilon}_{xx}$, $\Delta B=k_0^2(\tilde{\varepsilon}_{zz}+\tilde{\varepsilon}_{yy})-(\delta\beta)^2/\tilde{\varepsilon}_{xx})/2$, $\Delta C=$ $=k_0^4(2\tilde{\varepsilon}_{zz}\tilde{\varepsilon}_{yy}-(\delta\beta)^2\tilde{\varepsilon}_{zz}/\tilde{\varepsilon}_{xx})-k_z^2k_0^2\tilde{\varepsilon}_{zz}(1-\tilde{\varepsilon}_{yy}/\tilde{\varepsilon}_{xx})$. We assume that $k_z\gg k_0$ and the additions are small compared to the quantities denoted with zeros. Let us start with examining the first approximate root $k_x^2\approx k_z^2\tilde{\varepsilon}_{zz}/\tilde{\varepsilon}_{xx}$. Approximate equality $n_z^2\approx 1-n_z^2\tilde{\varepsilon}_{zz}/\tilde{\varepsilon}_{xx}$ (i. e., $\tilde{\varepsilon}_{zz}/\tilde{\varepsilon}_{xx}\approx -1$) should hold for the second DE. Assuming that the cyclotron frequency is high ($\omega_H^2\gg\omega_p^2/(\varepsilon_d(1-\delta)/\delta+\varepsilon_L)$), we find $\omega^2\approx\omega_H^2$ or $\omega^2\approx\omega_p^2/[2\varepsilon_d(1-\delta)/\delta+2\varepsilon_L]$. With low cyclotron frequency $\omega_H^2\ll\omega_p^2/(\varepsilon_d(1-\delta)/\delta+\varepsilon_L)$ we obtain either $\omega^2\approx\omega_p^2/[\varepsilon_d(1-\delta)/\delta+\varepsilon_L]$, or $\omega^2\approx\omega_H^2/2$. With the first term of the expansion with respect to a small parameter taken into account, the k_{x+}^2 and k_{x-}^2 quantities

may now be presented as

$$k_{x+}^2 = -k_z^2\tilde{\varepsilon}_{zz}/\tilde{\varepsilon}_{xx} + \Delta B + \frac{k_z^2(1-\tilde{\varepsilon}_{zz}/\tilde{\varepsilon}_{xx})}{2}\frac{4B_0\Delta B + 4(\Delta B)^2 - 2\Delta C}{k_z^4(1-\tilde{\varepsilon}_{zz}/\tilde{\varepsilon}_{xx})},$$

$$k_{x-}^2 = -k_z^2 + \Delta B - \frac{k_z^2(1-\tilde{\varepsilon}_{zz}/\tilde{\varepsilon}_{xx})}{2}\frac{4B_0\Delta B + 4(\Delta B)^2 - 2\Delta C}{k_z^4(1-\tilde{\varepsilon}_{zz}/\tilde{\varepsilon}_{xx})}.$$

The second case is of interest to us. Switching to decelerations, we obtain

$$n_x^2 \approx -n_z^2 + \frac{2\tilde{\varepsilon}_{yy} - (\delta\beta)^2[2+\tilde{\varepsilon}_{zz}/\tilde{\varepsilon}_{xx}]/\tilde{\varepsilon}_{xx} + \tilde{\varepsilon}_{zz}(3\tilde{\varepsilon}_{yy}+\tilde{\varepsilon}_{zz})/\tilde{\varepsilon}_{xx}}{2} - \frac{(\tilde{\varepsilon}_{zz}-\tilde{\varepsilon}_{yy})^2 + [(\delta\beta)^2/\tilde{\varepsilon}_{xx} - 2\tilde{\varepsilon}_{yy}](\delta\beta)^2/\tilde{\varepsilon}_{xx}}{2n_z^2}.$$

Inserting this result into the DE, we find

$$n_z^2 \approx \frac{(\tilde{\varepsilon}_{zz}-\tilde{\varepsilon}_{yy})^2 + \lfloor(\delta\beta)^2/\tilde{\varepsilon}_{xx} - 2\tilde{\varepsilon}_{yy}\rfloor(\delta\beta)^2/\tilde{\varepsilon}_{xx}}{2\tilde{\varepsilon}_{yy} - (\delta\beta)^2(2+\tilde{\varepsilon}_{zz}/\tilde{\varepsilon}_{xx})/\tilde{\varepsilon}_{xx} + \tilde{\varepsilon}_{zz}(3\tilde{\varepsilon}_{yy}+\tilde{\varepsilon}_{zz})/\tilde{\varepsilon}_{xx} - 2}. \quad (8)$$

This is true only for large decelerations. If the δ value is rather small,

$$n_z^2 \approx \frac{\tilde{\varepsilon}_{xx}(\tilde{\varepsilon}_{zz}-\tilde{\varepsilon}_{yy})^2}{2\tilde{\varepsilon}_{yy}\tilde{\varepsilon}_{xx} + 3\tilde{\varepsilon}_{yy}\tilde{\varepsilon}_{zz} + \tilde{\varepsilon}_{zz}\tilde{\varepsilon}_{zz} - 2\tilde{\varepsilon}_{xx}}.$$

The denominator should be close to zero to obtain a large deceleration. It is easy to find frequencies at which this condition is fulfilled. In the case of the first DE, $n_z^2 = 1 - n_{x\pm}^2/\tilde{\varepsilon}_{zz}^2$, a slow MP is obtained at $\tilde{\varepsilon}_{zz}\tilde{\varepsilon}_{xx} < 0$ and $\tilde{\varepsilon}_{zz} \approx 1$. The latter is feasible within a narrow band at $\omega \approx \omega_p/\sqrt{\varepsilon_L - \varepsilon_d + (\varepsilon_d - 1)/\delta}$. At $\varepsilon_d \sim \varepsilon_L \sim 10$ and small $\delta \sim 10^{-4}$, this frequency may be fairly low (on the order of $0.3\omega_p \cdot 10^{-2}$). Inserting $\tilde{\varepsilon}_{zz} = 1$ into (8), we find deceleration $n_z \approx \varepsilon_d/\sqrt{2\varepsilon_d + (3\varepsilon_d)/\tilde{\varepsilon}_{xx}}$.

3. Numerical results and discussion

Note that all the above results also apply to the case of complete filling $\delta = 1$. All depolarization coefficients are then removed from the relations, and DC (5) of a semiconductor or metal in a magnetic field is obtained. The DE solution in this case was discussed in [1]. The results for thin conducting metal or semiconductor layers on a substrate were also presented there. To obtain a slow MP, one needs to achieve sufficiently high CF (and low CR) values. The PF also needs to be reduced. This problem is solved by adjusting the carrier concentration in semiconductor inclusions and selecting a material with a low effective mass to obtain a PF in the THz range. The magnetic field induction should then be on the order of 1 T, which is typical of beam-focusing magnetic systems of TWTs based on rare-earth permanent magnets. At 1 T, $\omega_H = 13.54$ THz for InSb. The CR and the intrinsic carrier concentration are reduced by cooling to cryogenic temperatures. The accompanying PF reduction is compensated for by doping. When doped heavily, *n*-InSb is similar to a metal, and its PF depends only weakly on temperature. With an effective electron mass of $0.013m_e$ and concentration $N_e = 10^{24}$ m^{-3} in a doped sample, we obtain PF $\omega_p = 56.6$ THz. Since the conductivity at this concentration is $\sigma = 1.76 \cdot 10^7$ S/m, the CR is $\omega_{co} = \omega_p^2\varepsilon_0 = 1.6$ GHz. These parameters are quite acceptable for a slow MP in the THz range.

Using the simple iteration method, we then solve two DEs

$$k_z^2 = k_0^2 - B(k_0^2, k_z^2) \mp D(k_0^2, k_z^2), \quad (9)$$

$$k_z^2 = k_0^2 - \frac{B(k_0^2, k_z^2) \mp D(k_0^2, k_z^2)}{\tilde{\varepsilon}_{zz}^2}, \quad (10)$$

and DE (6). Four branches are possible for (9) and (10). Algebraic values of square root D found in (9) and (10) should be used in the calculation of k_x^2. Figure 2 presents the results for a structure with *n*-InSb, which converged with a relative error no worse than 10^{-14} in two iterations. The branches are denoted as *1, 2* for (9) and *3, 4* for (10); $k_x^2 = B \pm D$, where the upper sign corresponds to *1* and *3*, and the lower sign corresponds to *2* and *4*. At low frequencies, a large deceleration and fairly high losses correspond to curve *2*; therefore, this MP cannot be excited and observed at low frequencies. As the frequency increases, MP *1* becomes fairly fast, although there are three narrow regions where its deceleration is large and decreases abruptly. The same is true for MP *2*. The difference is that it is decelerated slightly at high frequencies, while MP *1* is fast. MPs *3* and *4* are characterized by a deceleration on the order of 1 at low frequencies. The deceleration increases at $\omega \approx \omega_H$, but then drops sharply to a fairly low level. Another two regions with such a transition are observed. At high frequencies, MP *3* is fast, and MP *4* has a deceleration equal to unity. The losses of all MPs are high in the regions of sharp transitions from large to small decelerations. However, regions with decelerations on the order of 10 and fairly low losses are found in the THz range.

CVD (chemical vapor deposition) diamond was used as a dielectric to plot Figures 2 and 3. It has high thermal conductivity and weak frequency dispersion, which is neglected. Figure 3 presents the results in the form of branches *3* and *4* of DE (10) for silver at room temperature. Branches *1* and *2* are not shown, since they are characterized by extreme decelerations and such high losses that make them irrelevant. Decelerations on the order of 4–5 are feasible for branches *3* and *4*, but only at a frequency on the order of 1 GHz. In addition, $n'' \approx n'$ in this case; i. e., the losses are high, and it is impossible to use such MPs to amplify an electron beam without loss compensation. The frequency of maximum deceleration corresponds to plasmon resonance, which contributes to an increase in losses. Thin metal films at low temperatures may be used to obtain slow and

weakly dissipative MPs [10]. The deceleration is much more significant in this case, and $n \sim 4$ at $n'' \ll n'$ in the region of moderate decelerations. The branches reveal a change in the sign of losses n'' in a number of regions, which is indicative of a transition from forward MPs to backward ones. Let us examine the equations for frequencies of such transitions

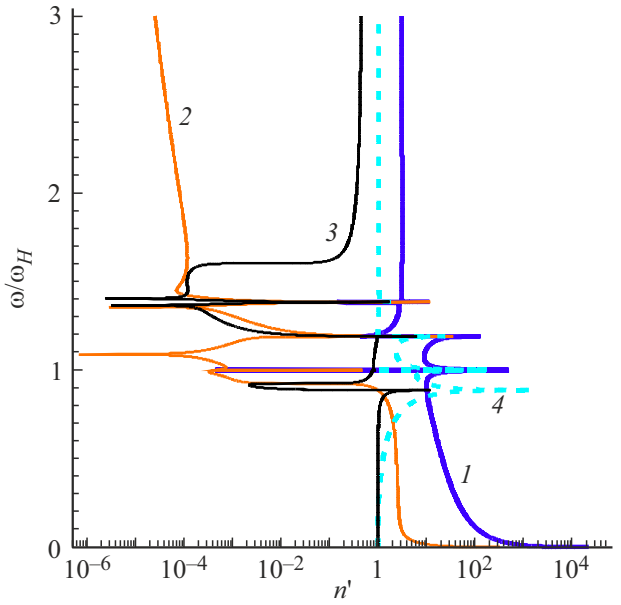

Figure 2. Normalized MP dispersion as a function of deceleration $n' = k_z'/k_0'$ in the structure shown in Figure 1, *a* with semiconducting *n*-InSb: $\varepsilon_L = 17.8$, $\varepsilon_d = 5.6$, $\delta = 0.1$, $\omega_p = 56.6$, $\omega_H = 13.54$, and $\omega_{co} = 0.0016$ (THz). Curves *1, 2* and *3, 4* correspond to Eqs. (9) and (10), respectively. (A color version of the figure is provided in the online version of the paper).

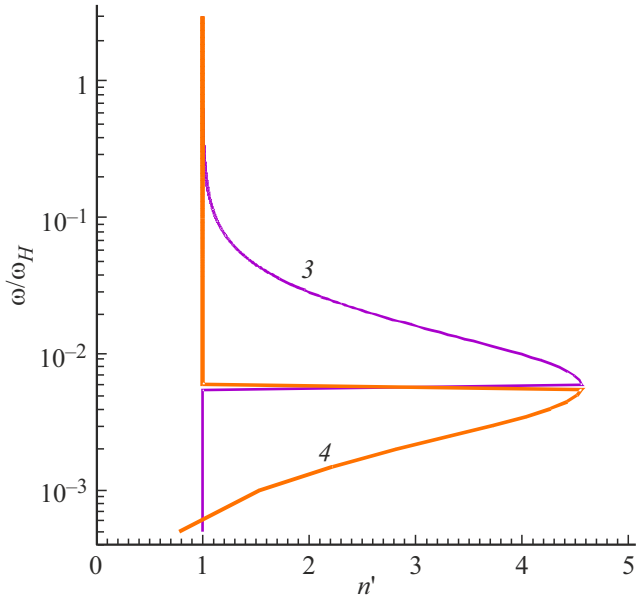

Figure 3. Normalized MP dispersion as a function of deceleration $n' = k_z'/k_0'$ in the structure shown in Figure 1, *a* with silver: $\varepsilon_L = 9.3$, $\varepsilon_d = 5.6$, $\delta = 0.1$, $\omega_p = 1.57 \cdot 10^{16}$, $\omega_H = 1.76 \cdot 10^{11}$, and $\omega_{co} = 3.56 \cdot 10^{13}$ (Hz). Curves *3, 4* correspond to Eq. (10).

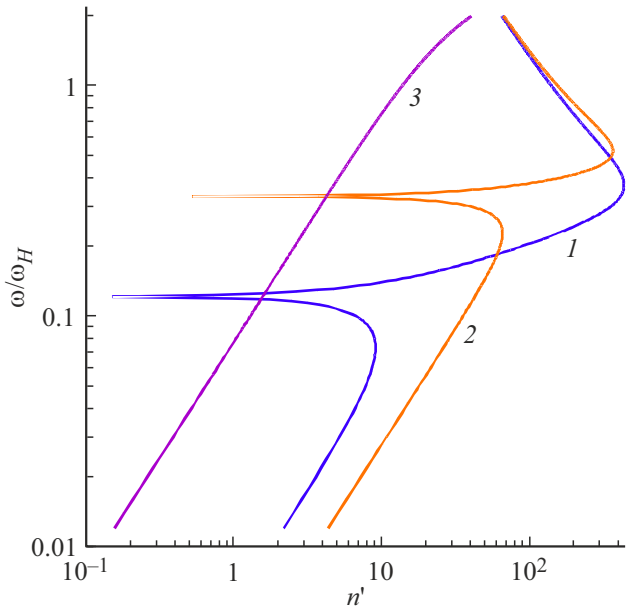

Figure 4. MP dispersion in an *n*-InSb film with $t = 10$ nm at $\omega_H = 13.5$, $\omega_{co} = 1$ calculated by formula (6) at different PFs ω_p: 18 (curve *1*), 25 (*2*), and 180 (*3*). The frequencies are given in THz.

using the example of DE (10). Setting $n = 1$, we find $B(k_0^2, k_0^2) \pm D(k_0^2, k_0^2) = 0$. Since this wave propagates with the velocity of light and zero losses, $k_{x\pm} = 0$; i.e., we obtain equations $B(k_o, k_0^2) = 0$ for $k_{x+} = 0$ and $C(k_0^2, k_0^2) = 0$ for $k_{x-} = 0$. In the case of a fast wave, $k_z \approx 0$, and the frequency is determined from $k_0^2 \tilde{\varepsilon}_{zz}^2 = B(k_0^2, k_0^2) \pm D(k_0^2, k_0^2)$. Dissipation effectively imposes a limit on large decelerations and enhances infinitely small ones; in the latter case, the wave is leaky (i.e., has high radiation losses).

Figure 4 shows the dispersion in a thin homogeneous *n*-InSb film with thickness $t = 10$ nm calculated using formula (6) with a plus sign at different doping levels. The frequencies of maxima and minima of n' increase with the carrier concentration and the plasma frequency. Decelerations in excess of 100 are feasible in thin semiconductor films. The losses are fairly low at decelerations on the order of 10, and this regime may be implemented within the range from 200 GHz to 1 THz in samples with a thickness of ~ 10 nm or more. Note that the introduction of an electrically thin CVD diamond substrate for such a film does not alter the dispersion in any significant way, but is structurally necessary and solves the issue of heat dissipation. A thin dielectric film with thickness d may be represented as surface conductivity $\sigma(\omega) = i\omega\varepsilon_0 d(\varepsilon_d - 1)$, and one needs just to add $-i\sigma(\omega)/\omega\varepsilon_0 = d(\varepsilon_d - 1)$ to components ε_{zz} and ε_{yy} (i.e., perform substitution $\varepsilon_L \to \varepsilon_L + \varepsilon_d - 1$) to account for it approximately in calculations.

Let us examine the DE solutions at ultralow frequencies with $\omega \to 0$. We have $\tilde{\varepsilon}_{xx}(0) = \varepsilon_L + \omega_p^2/\omega_H^2 \gg 1$ and $\beta^2(0) = \omega_p^4/(\omega_H^2\omega^2) \gg 1$, and quantities $\tilde{\varepsilon}_{zz}(0) \approx -\omega_p^2/(\omega\omega_c)$, $B(0) = -\left(k_z^2\tilde{\varepsilon}_{zz}(0)/\tilde{\varepsilon}_{xx}(0) + \delta^2 k_p^2\omega_p^2/\left(\omega_H^2\tilde{\varepsilon}_{xx}(0)\right)\right)/2$, and

$C(0) = -k_z^4\big(\tilde{\varepsilon}_{zz}(0)/\tilde{\varepsilon}_{xx}(0)\big)$ are large in magnitude (notably, $D(0, k_z^2) \approx B(0)\big(1 - C(0)/(2B^2(0))\big)$). Two roots $k_x^2 \approx 2B(0) - C(0)/\big(2|B(0)|\big)$ and $k_x^2 \approx -C(0)/\big(2|B(0)|\big)$ are obtained. If the value of $-C(0)/2|B(0)|$ is small, $k_z^2 \approx 2B(0)$ and $k_z \approx (1-i)\delta k_p\sqrt{\omega\omega_c}/\big(\sqrt{2\omega_H}\big)$ are found for the first branch; i.e., this MP is highly dissipative and fast at ultralow frequencies. At $\omega\omega_c \sim \omega_H^2$ and large k_p, its deceleration may be significant, and it is then determined from equation $k_z^2 + \tilde{\varepsilon}_{xx}\alpha k_z/\tilde{\varepsilon}_{zz} + \tilde{\varepsilon}_{xx}\alpha^2/\tilde{\varepsilon}_{zz} = 0$, where $\alpha^2 = \delta^2 k_p^2\omega_p^2/\big(\omega_H^2\tilde{\varepsilon}_{xx}(0)\big)$. This equation characterizes a dissipative MP. The second branch has $k_z^2 \approx k_0^2 + C(0)/\big(2|B(0)|\big)$, and the MP is fast if $-C(0)/|B(0)|$ is small: $k_z^2 \approx k_0^2$. If $-C(0)/|B(0)|$ is large, $k_z^2 = -i\delta^2 k_0 k_c\omega_p^2/(2\omega_H^2)$. Its deceleration $n = (1-i)\delta\omega_p/(2\omega_p)\sqrt{\omega_c/\omega}$ is inversely proportional to the square root of frequency. This condition may be satisfied at $\omega \ll \delta^2\omega_p^2\omega_c/(4\omega_H^2)$, and the MP is dissipative. Since $\tilde{\varepsilon}_{zz}^2$ is large in magnitude, approximate equality $k_z \approx k_0$ always holds true at low frequencies in the third and fourth branches. At IR and optical frequencies, the magnetic field has a weak effect, and a common PP with $n \approx \sqrt{\tilde{\varepsilon}_{zz}/(\tilde{\varepsilon}_{zz}+1)}$ disturbed by the magnetic field is observed.

4. Conclusion

The simplest artificial media made of conducting (semiconductor and metallic) elements (meta-atoms) and a thin semiconductor film in a strong external magnetic field were examined as waveguide structures for MPs of THz and microwave ranges. These MP waveguides may act as millimeter and THz slow-wave systems that do not require the fabrication of combs and other structures necessitating the use of MEMS-type technology. THz waveguides of this kind also allow one to implement magnetic control of dispersion. Spasers in the form of optically pumped graphene sheets or active semiconductor structures hold promise as a means for loss reduction. It is convenient to use the CVD technology combined with other methods for production of layered planar thin-film structures to fabricate structures of the type shown in Figure 1, *a*.

Funding

This study was supported by the Ministry of Education and Science of the Russian Federation (state assignment FSR-2023-0008).

Conflict of interest

The author declares that he has no conflict of interest.

Appendix

Let us use the effective DC components, which take the form

$$\tilde{\varepsilon}_{xx} = \varepsilon_d\,\frac{\varepsilon_d + (L_x + \delta(1-L_x))(\varepsilon_\perp - \varepsilon_d)}{\varepsilon_d + L_x(1-\delta)(\varepsilon_\perp - \varepsilon_d)}$$

$$\approx \varepsilon_d[1 + \delta(\varepsilon_\perp/\varepsilon_d) - 1)],$$

$$\tilde{\varepsilon}_{yy} = \varepsilon_d\,\frac{\varepsilon_d + (L_y + \delta(1-L_y))(\varepsilon_\perp - \varepsilon_d)}{\varepsilon_d + L_y(1-\delta)(\varepsilon_\perp - \varepsilon_d))}$$

$$\approx \varepsilon_d + \delta\varepsilon_d(1 - \varepsilon_d/\varepsilon_\perp),$$

$$\tilde{\varepsilon}_{zz} = \varepsilon_d + \delta(\varepsilon - \varepsilon_d),$$

$$\tilde{\varepsilon}_{xy}(\omega) = -\tilde{\varepsilon}_{yx}(\omega) = -i\delta\beta. \qquad (A.1)$$

The Maxwell's equations with an MP propagating along axis x ($k_y = 0$) are written as

$$\begin{pmatrix}\tilde{\varepsilon}_{xx} & -i\delta\beta & 0\\ i\delta\beta & \tilde{\varepsilon}_{yy} & 0\\ 0 & 0 & \tilde{\varepsilon}_{zz}\end{pmatrix}\begin{pmatrix}E_x\\E_y\\E_z\end{pmatrix} = \frac{1}{k_0}\begin{pmatrix}0 & k_z & 0\\ -k_z & 0 & k_x\\ 0 & -k_x & 0\end{pmatrix}\begin{pmatrix}h_x\\h_y\\h_z\end{pmatrix}, \qquad (A.2)$$

$$\begin{pmatrix}h_x\\h_y\\h_z\end{pmatrix} = \frac{1}{k_0}\begin{pmatrix}0 & -k_z & 0\\ k_z & 0 & -k_x\\ 0 & -k_x & 0\end{pmatrix}\begin{pmatrix}E_x\\E_y\\E_z\end{pmatrix} = \begin{pmatrix}-n_z E_y\\ n_z E_x - n_x E_z\\ n_x E_y\end{pmatrix}. \qquad (A.3)$$

Here and elsewhere, $n_x = k_x/k_0$ and $n_z = k_z/k_0$. Normalized magnetic field $\mathbf{h} = \eta_0\mathbf{H}$ with the dimension of electric field (V/m), where $\eta_0 = \sqrt{\mu_0/\varepsilon_0}$ is the wave impedance of vacuum, was introduced for convenience. Common factor $\exp(i\omega t - ik_z z)$ is hereinafter omitted. Inserting (A.3) into (A.2), we obtain equations

$$\begin{pmatrix}k_0^2\tilde{\varepsilon}_{xx} - k_z^2 & -i\delta\beta k_0^2 & -k_x k_z\\ i\delta\beta k_0^2 & k_0^2\tilde{\varepsilon}_{yy} - k_x^2 - k_z^2 & 0\\ -k_x k_z & 0 & k_0^2\tilde{\varepsilon}_{zz} - k_z^2\end{pmatrix}\begin{pmatrix}E_x\\E_y\\E_z\end{pmatrix} = 0. \qquad (A.4)$$

Equating the determinant in (A.4) to zero, we find Fresnel dispersion equation

$$(k_0^2\tilde{\varepsilon}_{xx}\tilde{\varepsilon}_{zz} - k_z^2\tilde{\varepsilon}_{zz} - k_x^2\tilde{\varepsilon}_{xx})(k_0^2\tilde{\varepsilon}_{yy} - k_z^2 - k_x^2)$$

$$-(\delta\beta)^2 k_0^2(k_0^2\tilde{\varepsilon}_{zz} - k_x^2) = 0. \qquad (A.5)$$

This equation yields $k_{x\pm}^2 = B \pm D$, $D = \sqrt{B^2 - C}$. Here,

$$B = (k_0^2\tilde{\varepsilon}_{zz} + k_0^2\tilde{\varepsilon}_{yy} - k_z^2 - k_z^2\tilde{\varepsilon}_{zz}/\tilde{\varepsilon}_{xx} - (\delta\beta)^2 k_0^2/\tilde{\varepsilon}_{xx})/2, \qquad (A.6)$$

$$C = (k_0^2\tilde{\varepsilon}_{zz} - k_z^2\tilde{\varepsilon}_{zz}/\tilde{\varepsilon}_{xx})(k_0^2\tilde{\varepsilon}_{yy} - k_z^2) - (\delta\beta)^2 k_0^4\tilde{\varepsilon}_{zz}/\tilde{\varepsilon}_{xx}. \qquad (A.7)$$

Inverting the matrix in (A.3), we find couplings $E_y = [\tilde{\varepsilon}_{xx}(n_x h_z - n_z h_z) - i\delta\beta n_z h_y]/\varepsilon_\tau^2$, $E_z = -n_x h_y/\tilde{\varepsilon}_{zz}$, $h_y = n_z E_x - n_x E_z = n_z\tilde{\varepsilon}_{zz}E_x/(\tilde{\varepsilon}_{zz} - n_x^2)$, $h_z = n_x E_y$, $h_x = -n_z E_y$, where $\varepsilon_\tau^2 = \tilde{\varepsilon}_{xx}\tilde{\varepsilon}_{yy} - (\delta\beta)^2$. Inserting magnetic components into

the electrical ones (and vice versa), we obtain tangential components

$$E_y = \alpha_{yx}E_x - \rho_{hz}h_x = -n_z\frac{\tilde{\varepsilon}_{xx}(\tilde{\varepsilon}_{zz}-n_x^2)h_x + ibn_z\tilde{\varepsilon}_{zz}E_x}{(\varepsilon_\tau^2-\tilde{\varepsilon}_{xx}n_x^2)(\tilde{\varepsilon}_{zz}-n_x^2)}, \tag{A.8}$$

$$E_z = \alpha_{zx}E_x = \frac{n_xn_z}{n_x^2-\tilde{\varepsilon}_{zz}}E_x, \tag{A.9}$$

$$h_y = y_{ez}E_x = \frac{n_z\tilde{\varepsilon}_{zz}}{\tilde{\varepsilon}_{zz}-n_x^2}E_x, \tag{A.10}$$

$$h_z = \beta_{zx}h_x - y_{hy}E_x = -n_xn_z\frac{\tilde{\varepsilon}_{xx}(\tilde{\varepsilon}_{zz}-n_x^2)h_x + ibn_z\tilde{\varepsilon}_{zz}E_x}{(\varepsilon_\tau^2-\tilde{\varepsilon}_{xx}n_x^2)(\tilde{\varepsilon}_{zz}-n_x^2)}. \tag{A.11}$$

The following coefficients were introduced here:

$$\alpha_{yx} = -n_z\frac{ibn_z\tilde{\varepsilon}_{zz}}{(\varepsilon_\tau^2-\tilde{\varepsilon}_{xx}n_x^2)(\tilde{\varepsilon}_{zz}-n_x^2)},$$

$$\rho_{hz} = n_z\frac{\tilde{\varepsilon}_{xx}(\tilde{\varepsilon}_{zz}-n_x^2)}{(\varepsilon_\tau^2-\tilde{\varepsilon}_{xx}n_x^2)(\tilde{\varepsilon}_{zz}-n_x^2)},$$

$$\beta_{zx} = -n_xn_z\frac{\tilde{\varepsilon}_{xx}(\tilde{\varepsilon}_{zz}-n_x^2)}{(\varepsilon_\tau^2-\tilde{\varepsilon}_{xx}n_x^2)(\tilde{\varepsilon}_{zz}-n_x^2)},$$

$$y_{hy} = n_xn_z\frac{ibn_z\tilde{\varepsilon}_{zz}}{(\varepsilon_\tau^2-\tilde{\varepsilon}_{xx}n_x^2)(\tilde{\varepsilon}_{zz}-n_x^2)}. \tag{A.12}$$

The normal components of fields in a metamaterial (at $x<0$) may be presented as $E_x(x) = = E_1^+\exp(ik_{x+}x)+E_1^-\exp(ik_{x-}x)$, $h_x(x)=h_1^+\exp(-ik_x^{(+)}x) - h_1^-\exp(ik_x^{(-)}x)$ (i. e., as a combination of two FE solutions k_{x+} and k_{x-} decaying with depth in the structure). The tangential components are determined with the use of (A.8)–(A.11). In the case of a finite layer, one should take into account the waves propagating in both directions along x. There are two DEs (6), (7) for a homogeneous layer of this kind.

References

[1] M.V. Davidovich. Quantum Electron., **47** (6), 567 (2017). DOI: 10.1070/QEL16272

[2] M.V. Davidovich. Opt. Spectrosc., **130** (10), 1263 (2022). DOI: 10.21883/EOS.2022.10.54863.3231-22

[3] F.K. Schulte. Surf. Sci., **55**, 427 (1976). DOI: 10.1016/0039-6028(76)90250-8

[4] A.E. Meyerovich, A. Stepaniants. Phys. Rev. B, **58** (19), 13242 (1998). DOI: 10.1103/PhysRevB.58.13242

[5] J. Brion, R. Wallis, A. Hartstein, E. Burstein. Phys. Rev. Lett., **28**, 145 (1972). DOI: 10.1103/PhysRevLett.28.1455

[6] P. Kumar, V.K. Tripathi. J. Appl. Phys., **114**, 053101 (2013). DOI: 10.1063/1.4817091

[7] R.K. Srivastav, A. Panwar. Optical Quant. Electron., **55**, 111 (2023). DOI: 10.1007/s11082-022-04299-y

[8] P. Kumar, M. Kumar, V. Tripathi. Optics Lett., **41**, 1408 (2016). DOI: 10.1364/OL.41.001408

[9] R.K. Srivastav, A. Panwar. Optik, **264**, 169363 (2022). DOI: 10.1016/j.ijleo.2022.169363

[10] M.V. Davidovich. JETP Lett., **119** (3), 186 (2024). DOI: 10.31857/S1234567824030066

[11] I.A. Kuznetsova, O.V. Savenko, P.A. Kuznetsov. Semiconductors, **54**, 1039 (2020). DOI: 10.1134/S106378262009016X

[12] A.A. Bulgakov, I.V. Fedorin. Techn. Phys., **56** (4), 510 (2011). DOI: 10.1134/S1063784211040098

[13] I.A. Kolmychek, I.V. Malysheva, V.B. Novikov, A.I. Maydykovskiy, A.P. Leontiev, K.S. Napolskii, T.V. Murzina. JETP Letters, **114** (11), 653 (2021). DOI: 10.1134/S0021364021230089

[14] M.V. Davidovich. Computer Optics, **45** (1), 48 (2021). DOI: 10.18287/2412-6179-CO-673

[15] M.V. Davidovich. Techn. Phys. Lett., **49** (1), 7–11. DOI: 10.21883/TPL.2023.01.55337.19196

[16] P.A. Belov, R. Marqués, S.I. Maslovski, I.S. Nefedov, M. Silveirinha, C.R. Simovski, S.A. Tretyakov. Phys. Rev. B, **67**, 113103 (2003). DOI: 10.1103/PhysRevB.67.113103

[17] P.A. Belov, C.R. Simovski, S.A. Tretyakov. Phys. Rev. E, **66**, 036610 (2002). DOI: 10.1103/PhysRevE.66.036610

[18] S.A. Tretyakov, S. Maslovski, P.A. Belov. IEEE Trans. AP, **51** (10), 2652 (2003). DOI: 10.1109/TAP.2003.817557

[19] C.R. Simovski, P.A. Belov. Phys. Rev. E, **70**, 046616 (2004). DOI: 10.1103/PhysRevE.70.04661

[20] P.A. Belov, C.R. Simovski. Phys. Rev. E, **72**, 026615 (2005). DOI: 10.1103/PhysRevE.72.026615

[21] P.A. Belov, C.R. Simovski, P. Ikonen. Phys. Rev. B, **71**, 193105 (2005). DOI: 10.1103/PhysRevB.71.193105

[22] P.A. Belov, Y. Hao, S. Sudhakaran. Phys. Rev. B, **73**, 033108 (2006). DOI: 10.1103/PhysRevB.73.033108

[23] P. Ikonen, P. Belov, C. Simovski, S. Maslovski. Phys. Rev. B, **73**, 073102 (2006). DOI: 10.1103/PhysRevB.73.073102

[24] P.A. Belov, M.G. Silveirinha. Phys. Rev. E, **73**, 056607 (2006). DOI: 10.1103/PhysRevE.73.056607

[25] A. Alú, M.G. Silveirinha, A. Salandrino, N. Engheta. Phys. Rev. B, **75**, 155410 (2007). DOI: 10.1103/PhysRevB.75.155410

[26] S.M. Rytov. Sov. Phys. JETP, **2** (3) 466 (1956).

[27] M.A. Ordal, L.L. Long, R.J. Bell, S.E. Bell, R.R. Bell, R.W. Alexander, Jr., C.A. Ward. Appl. Optics, **22** (7), 1099 (1983). DOI: 10.1364/ao.22.001099

[28] I.I. Berchenko, M.V. Pashkovskii. Phys. Usp., **19** (6), 462 (1976). DOI: 10.1070/PU1976v019n06ABEH005265]

Translated by D.Safin